Desalination and Water Treatment
www.deswater.com

doi:10.5004/dwt.2017.20207

66 (2017) 184–194
March

The distribution and characteristics of dissolved organic matter fractions in urban rivers during icebound season

Shuang Xue[a], Ying Liu[a], Yang Wen[a], Fayun Li[a,b,*]

[a]*School of Environment, Liaoning University, Shenyang, China, email: xueshuang666@sina.com (S. Xue), yingeraichitian@sina.com (Y. Liu), jeankie@126.com (Y. Wen)*
[b]*National & Local United Engineering Laboratory of Petroleum Chemical Process Operation Optimization and Energy Conservation Technology, Liaoning Shihua University, Fushun, Liaoning province, China, Tel. +86-2462202248, Fax +86-2462204818, email: ldxslw666@126.com (F. Li)*

Received 27 April 2016; Accepted 29 August 2016

ABSTRACT

Dissolved organic matter (DOM) in surface waters has important implication for water quality, and also plays an important role in the distribution, bioavailability, and toxicity of pollutants in waters. The distribution, spectroscopic characteristics and chlorine reactivity of DOM fractions in the North Canal in Shenyang during icebound season were investigated. DOM was fractionated using XAD resins into five fractions: hydrophobic acid (HPO-A), hydrophobic neutral (HPO-N), transphilic acid (TPI-A), transphilic neutral (TPI-N) and hydrophilic fraction (HPI). The results showed that dissolved organic carbon (DOC) concentrations in river waters were relatively high during icebound season. DOC values of the bulk DOM, HPO-A, TPI-A and TPI-N in ice phase were lower than those corresponding values in liquid phase. The variation trend of absorbance of ultraviolet light at 254 nm (UV_{254}) along the direction of water was inconsistent with that of DOC in both liquid and ice phases. HPO-A and TPI-A were the dominant ultraviolet (UV)-absorbing compounds in both liquid and ice phases. The variation trend of fluorescent materials in ice phase along the direction of water was similar to that in liquid phase. HPO-A, HPO-N and TPI-N were the main trihalomethane precursors in both liquid and ice phases. Trihalomethane formation potential (THMFP) of HPO-A, TPI-A, HPO-N and TPI-N in ice phase was lower than that in liquid phase. Such knowledge can assist in our understanding of DOM dynamics in urban rivers during icebound season, and thus provides improved insight into the development of effective water quality management.

Keywords: Icebound season; Urban river; Dissolved organic matter; Liquid phase; Ice phase

1. Introduction

With the speeding up of urbanization and improvement of people's living standard, people have higher and higher requirements for water supply, and dissolved organic matter (DOM) in water gradually become hot topics in the study of environmental water quality and water treatment technology. It is a major concern in drinking water treatment since it causes adverse esthetic qualities such as color, taste, and odor. In the process of water treatment, the existence of DOM will affect the effect of coagulation, accelerate the blocking of filter bed and filter membrane. Furthermore, past researches have shown that the chlorination process of natural water containing DOM may cause the production of harmful disinfection by-products (DBPs) such as trihalomethanes (THMs) and haloacetic acids (HAAs), which are concerned for human health security [1,2]. Because of their complex polymeric properties, it is often necessary to isolate DOM for a better understanding of its role in water chemistry. The XAD resin method has been reported in many applications for fractionation of DOM and is generally considered as the state-of-art method at present for such fractionation [3]. The fractionation of the bulk DOM into some well-defined

*Corresponding author.

subcomponents allowed a thorough investigation of the chlorine reactivity and spectral characterization of the DOM fractions [4,5].

Fluorescence spectroscopy has been applied for characterizing fluorescence properties of DOM for several decades. This technique provides important information on the chemical properties of the fluorescing fraction of organic matter. It is a versatile, simple, rapid and sensitive method requiring only a small volume of sample [6]. The fluorescence regional integration (FRI) technique proposed by Chen et al. [7] is used to analyze quantitatively all the wavelength-dependent fluorescence intensity data from excitation-emission matrix (EEM) spectra [8]. EEM spectra were divided in five excitation–emission regions using consistent excitation and emission wavelength boundaries, and the quantitative analysis included the integration of the volume beneath each region, which represents the cumulative fluorescence response of DOM with similar properties [7].

Urban rivers are rivers or river sections that originate in cities or flow through urban areas. They generally include canals which are artificially excavated, but have the characteristics of natural rivers after many years of evolution [9]. With the rapid development of urban economy and the growing of urban scale, urban sewage emissions continue to increase, and urban rivers which act as important resource and sewage receivers in cities have been seriously polluted. Some urban rivers are black and smelly all year round, and seriously affect the ecology and landscape in cities [10]. Currently, the pollution status, causes and variations of heavy metals and organic pollutants in urban rivers have been investigated by many researchers [11]. However, these studies focused on the non freezing period. The phenomenon that waters freeze in cold areas is universal. The winter is long and very cold in the north of China, where large bodies of water, such as rivers, lakes, and reservoirs, are ice-covered for 3~5 mo each year. For rivers during icebound season, the hydrological characteristics and other factors affecting the reduction of pollutants in waters are different from those during non freezing period. As a result, the distribution, characteristics and fate of pollutants in rivers during icebound season might be different from those during non freezing period [12,13]. DOM in urban rivers plays important roles in the ecological environment and health of residents in cities. However, the distribution and characteristics of DOM in urban rivers during icebound season still remain unclear. The objectives of this study are, therefore, to investigate the distribution, spectroscopic characteristics and chlorine reactivity of DOM fractions in both liquid and ice phases in urban rivers during icebound season.

2. Materials and methods

2.1 Sampling method

The North Canal is located in the north of Shenyang. It is an artificial irrigation channel excavated in 1914, with the length of 27.7 km and the width of 15~25 m. The North Canal is the longest river in the round-the-city water systems in Shenyang. The North Canal flow is made up freshwater from the Hunhe River as well as treated and/or untreated domestic wastewater. The Beibu Wastewater Treatment Plant effluent contributes 7~28% of the flow.

As shown in Fig. 1, there were six sampling sites along the North Canal, and the flow direction of water was from the sampling point 1 to 6. The locations and geographical conditions of the six sampling points were shown in Table 1. The water and ice samples were collected on 27 December 2014, and on 10 and 25 January during icebound season in 2015, respectively. The whole thick ice samples were collected with the stainless round ice auger, and then put into the stainless barrels. Water samples were collected using a stainless water sample collector from the holes drilled with the ice auger, and put into acid-cleaned and pre-conditioned polypropylene buckets. Water temperature was measured in situ with a thermometer. Dissolved oxygen (DO) of all water samples was determined in field using a portable dissolved oxygen analyzer (Liance SIN-DO30, Hangzhou, China). Samples were immediately delivered to the laboratory and stored at 4°C. The three samples collected at the same sampling point were set as one sample by equal volume mixing. The ice samples colleted at 1, 2, 3, 4, 5 and 6 sampling points were designated as B1, B2, B3, B4, B5, and B6, respectively. Similarly, the waters colleted at 1, 2, 3, 4, 5 and 6 sampling points were designated as S1, S2, S3, S4, S5, and S6, respectively. The general water quality data for S1~S6 water samples and B1~B6 ice samples (all ice samples thawed at room temperature and then subjected to water quality measurements) were shown in Table 2. In addition, water samples were also collected

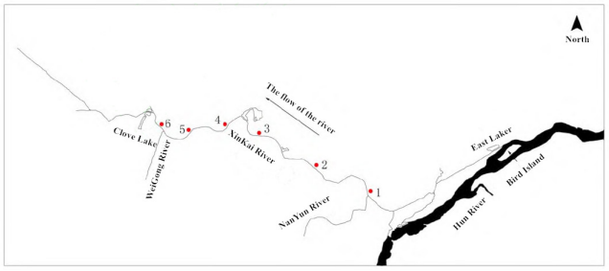

Fig. 1. Locations of the sampling points along the North Canal.

Table 1
The locations and geographical conditions of the six sampling points

Sampling points	Sampling sites	Coordinates	Distance to the source (km)
1	Hemu Road Bridge	123°30′48″E, 41°48′50″N	9.69
2	Desheng Bridge	123°29′14″E, 41°49′4″N	12.28
3	Liaohe Bridge	123°26′39″E, 41°50′24″N	17.07
4	Changjiang Bridge	123°25′4″E, 41°50′47″N	19.69
5	Taiping Bridge	123°23′13″E, 41°50′23″N	23.08
6	Dayu Bridge	123°22′27″E, 41°50′9″N	24.81

Table 2
General water quality data for water and ice samples collected at the six sampling points along the North Canal during icebound season

Sampling points	Sample name	Conductivity (ms/cm)	Temperature (°C)	pH	DO (mg/L)	NH_3–N (mg/L)	DOC (mg/L)	UV_{254} (m^{-1})
	Water samples/Ice samples	Water samples/Ice samples	Water samples/Ice samples	Water samples/Ice samples	Water samples/Ice samples	Water samples/Ice samples	Water samples/Ice samples	Water samples/Ice samples
1	S1/B1	720.0/233.0	0/–	7.1/6.7	5.20/–	1.5/0.1	6.4/4.0	7.8/6.1
2	S2/B2	696.0 /90.0	0/–	7.1/7.4	4.23/–	1.3/0.3	5.9/2.1	7.6/3.4
3	S3/B3	705.0/323.0	0/–	6.4/7.0	2.56/–	8.4/0.2	9.5/7.6	8.8/8.0
4	S4/B4	698.0/115.0	0/–	6.5/8.5	2.40/–	6.7/0.2	9.3/5.1	8.4/8.5
5	S5/B5	706.0/115.0	0/–	7.1/8.5	2.21/–	1.4/0.3	6.7/1.2	12.2/11.3
6	S6/B6	883.0/351.0	0/–	6.9/7.6	1.08/–	1.6/0.3	12.2/1.9	14.1/13.3

at the sampling point 6 biweekly in 2014, to investigate monthly variations of dissolved organic carbon (DOC) in water of the North Canal.

2.2 DOM fractionation

According to the different adsorption properties of XAD-8/XAD-4 resin, DOM was fractionated into five classes: hydrophobic acid (HPO-A), hydrophobic neutral (HPO-N), transphilic acid (TPI-A), transphilic neutral (TPI-N) and hydrophilic fraction (HPI) [7,14]. The DOM fractionation method was as follows: samples were filtered through 0.45 μm filter, acidified to pH 2, and then passed through two columns in series containing XAD-8 and XAD-4 resins. After all the samples were run through the columns, each column was separately back eluted with 0.1 mol/L sodium hydroxide (NaOH). The eluate from XAD-8 is defined as HPO-A and the eluate from XAD-4 is defined as TPI-A. Both HPO-A and TPI-A were desalted using cation exchange resin and freeze-dried using a vacuum freeze dry system. HPO-N and TPI-N are those compounds that adsorb onto XAD-8 and XAD-4 resins, respectively but are not dissolved during back elution with NaOH. They were desorbed from the XAD resins using a 75% acetonitrile/25% Milli-Q water solution. Acetonitrile was subsequently removed using rotary-evaporation and the resin isolates were lyophilized. HPI is the carbon in the XAD-4 effluent, which was desalted using cation/anion exchange resin and then further concentrated using rotary evaporator to reduce liquid volume prior to lyophilization. DOC, absorbance of ultraviolet light at 254 nm (UV_{254}), fluorescence spectra and trihalomethane formation potential (THMFP) of the fractionated samples were measured.

2.3 THMFP measurement

THMFP measurements were performed according to Standard Method 5710B. All samples were adjusted to a pH of 7 ± 0.2, buffered with a phosphate solution, and chlorinated with an adequate excess amount of concentrated sodium hypochlorite (NaClO), to assure a residue concentration of free chlorine of about 3~5 mg/L at the end of the reaction period (requiring 7d at 25 ± 2°C). At the end of this reaction period, the residual chlorine was immediately quenched with sodium sulfite (Na_2SO_3) and analysis of trihalomethane (THM) was conducted without delay. THMs were extracted with methyl tertbutyl ether (MTBE) from the chlorinated samples using a modified EPA method 551.1 and analyzed by gas chromatography with an electron capture detector (GC/ECD, CP-3800, Varian, Palo Alto, California, USA).

2.4 Analysis

DOC concentration for DOM fractions was analyzed using a Shimadzu TOC-5000 Total Organic Carbon Analyzer (Shimadzu, Kyoto, Japan) with auto-sampler.

UV_{254} was measured with a Cary 50 ultraviolet-visible (UV–VIS) spectrophotometer (Varian, Palo Alto, California, USA). Specific ultraviolet light absorbance (SUVA) was calculated as (UV_{254}/DOC) × 100.

Fluorescence spectra were obtained with a Cary Eclipse spectrofluorometer (Varian, Palo Alto, California, USA). Regulating water pH value of 7, and then loaded into 1 cm quartz fluorescent sample pool with three-dimensional fluorescence spectrometry. Slits were set to 5 nm for both excitation and emission and scan speed was set at 1200 nm/min. The excitation (Ex) wavelength was increased from 220 to 400 nm (5-nm intervals), whereas the emission (Em) wavelength range was fixed from 290 to 550 nm (1-nm intervals). All data were normalized to the intensity of the water Raman scatter peak, determined daily with freshly distilled water, and corrected for inner filter effects by means of absorbance at 254 nm.

The EEM spectra were divided into five regions which represented specific fractions of DOM. The five regions were as follows: Regions I (Ex: 220~250 nm/Em: 290~330 nm) and II (Ex: 220~250 nm/Em: 330~380 nm) recognized as belonging to aromatic protein-like fluorescence, Region III (Ex: 220~250 nm/Em: 380~550 nm) associated with fulvic acid-like fluorescence, Region IV (Ex: 250~400 nm/Em: 290~380 nm)related to soluble microbial byproduct-like (SMP-like) florescence, and Region V (Ex: 250~400 nm/Em: 380~550 nm) assigned to humic acid-like fluorescence. The quantitative analysis of EEMs was conducted follow-

ing the FRI technique proposed by [7], which integrate the volume beneath EEM spectra. According to [7], normalized region-specific EEM volume ($\Phi_{i,n}$) and cumulative EEM volume ($\Phi_{T,n}$) were calculated as follows:

$$\Phi_{i,n} = MF_i \int I(Ex/Em)dExdEm$$

$$\Phi_{T,n} = \sum_{i=1}^{5} \Phi_{i,n}$$

where Φ_i is the volume beneath region "*i*" of the EEM and MF_i is the multiplication factor for each region, which was equal to the inverse of the fractional projected excitation-emission area [15].

To eliminate the Rayleigh scattering interference [16], the intensity values at points where the emission wavelength was the same as or twice the excitation wavelength, as well as those adjacent to them (±20 nm emission wavelength at the same excitation wavelength), were excised from the scan data and the excised values were replaced with zero. In addition, this procedure was also applied to the data points in EEMs with an emission wavelength (the excitation wavelength or) twice the excitation wavelength. All data points whose value had been replaced with zero were excluded when counting the number of EEM data points per region and subsequently calculating projected excitation-emission area and MF_i [17].

2.5 Statistical analyses

Statistical analyses including mean value, standard deviations, and correlation coefficients were performed with SPSS 13.0 software. Significance of the correlations in the statistics was evaluated using *p*-values.

3. Results and discussion

3.1 Monthly variations of DOC in river waters

As shown in Fig. 2, the DOC values in river waters were relatively high during icebound season, with values of 8.2 mg/L, 8.7 mg/L, 7.8 mg/L in December, January, and February, respectively. The DOC values in these three months were 6.4~62.9% higher than those in the other nine months. The removal efficiency of organic pollutants in sewage treatment plants in winter is lower than other seasons, so that the quantity of organic pollutants which enter the urban rivers in winter is higher than other seasons [18]. Moreover, frozen period and dry season of river occur at the same time, leading to the decrease of river flow which weakens the dilution of pollutants in rivers [19]. Water temperature is low in this season, which directly affects the degradation of pollutants by microorganisms [20]. The water surface is covered with ice, resulting in the halt of reaeration progrecess in river waters, and therefore the DO concentration in river waters is at the lowest level [20]. High concentration of pollutants, as well as low DO concentration, leads to a bad state of river water quality during icebound season.

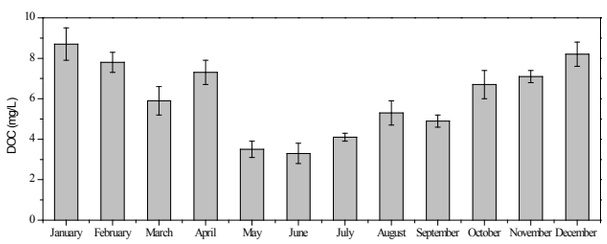

Fig. 2. Monthly variations of DOC in the North Canal waters.

3.2 DOM-fraction distribution in liquid and ice phase

As shown in Table 2, DOC of unfractionated water samples did not gradually decreased along the direction of water. Among the six water samples, the highest DOC value occurred in S6 (12.2 mg/L), and the relatively low DOC values were observed in S1 (6.4 mg/L), S2 (5.9 mg/L) and S5 (6.7 mg/L). The DOC values of S3 and S4 were 9.5 mg/L and 9.3 mg/L, respectively. The sampling points 1 and 2 were located in the suburbs with less pollution, so the DOC values of S1 and S2 was relatively low. The DOC values of S3 and S4 were relatively higher, which might be attributed to the input of a considerable amount of treated or untreated wastewaters. As expected, the DOC value of S5 decreased relative to S4. The sewage discharge was not found along the river reach from S4 to S5, and the DOC decrease was possibly due to the role of adsorption and precipitation. The sampling point 6 was located 5 m downstream of a sewage outfall, so the DOC value of S6 was quite high. Hou and Li [12] investigated the biochemical oxygen demand (BOD)-DO dynamics for rivers in northern China during icebound season. They found that BOD values decreased along the Tumen River, and believed that the BOD attenuation might be mainly attibuted to the precipitation of oxygen consumption substances.

As shown in Fig. 3a and Table 2, except for HPO-A and HPO-N which slightly increased along the river reach from S3 to S4, HPO-A, HPO-N, TPI-A and TPI-N in liquid phase followed the pattern of the bulk DOM along the North Canal; DOC decreased significantly along the river reaches from S1 to S2 and from S3 to S5, whereas there were obvious DOC increases observed along the river reaches from S2 to S3 and from S5 to S6 due to sewage discharge. On the other hand, the DOC values of HPI in liquid phase were in the range of 0.2~0.3 mg/L, showing smaller extent of DOC variation along the North Canal. For HPI, there were not obvious DOC increases found along the river reaches from S2 to S3 and from S5 to S6, suggesting low content of this fraction in wastewaters discharged in these river reaches.

As shown in Fig. 3b and Table 2, except for HPI which increased along the river reach from S1 to S2, the variation trend of the bulk DOM as well as of all the five fractions in ice phase was the same with that of the bulk DOM in liquid phase. The results was consistent with those obtained from our previous study investigating the partitioning behavior of DOM in liquid and ice phases during the freezing processes of water by means of indoor simulation experiments [21]. It was found in our study that the concentration of DOM in feed water significantly affected the partitioning of DOM in liquid and ice phases during freezing processes of water; the higher the DOM concentration in feed water,

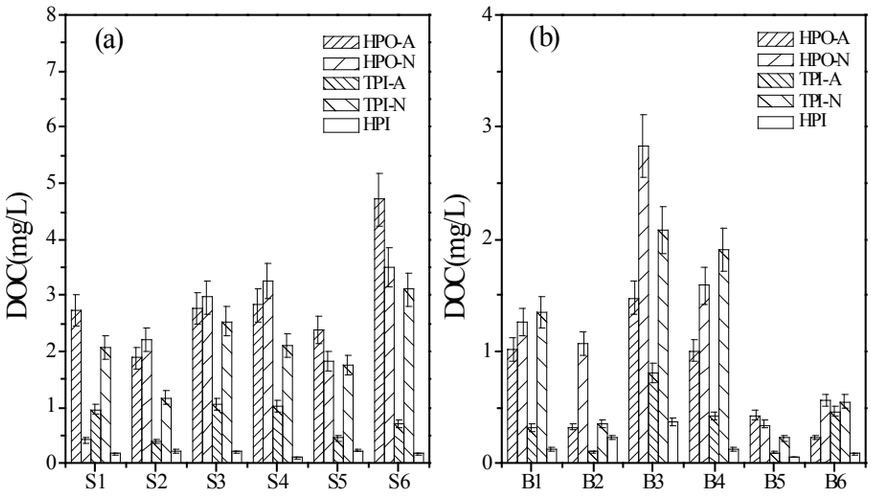

Fig. 3. DOC concentrations for DOM fractions in water (a) and ice (b) samples in the North Canal during icebound season.

the more DOM was incorporated in the ice formed during freezing [21].

As shown in Table 2, the bulk DOC in ice phase was 0.2~0.8 times that in liquid phase. The results agreed with a long known fact that when water freezes up, the ice contains less impurity than the water from which it is formed. This is because when ice is crystallized, the crystal is built up by pure water leaving the foreign bodies in the remaining liquid phase [22]. As shown in Fig. 3, except for DOC value of HPO-N in liquid phase lower than that in ice phase at the sampling point 1, the DOC values of HPO-A,HPO-N, TPI-A and TPI-N in liquid phase were all higher than those in ice phase at each sampling point. For example, the DOC values of HPO-A in liquid phase were 1.9~20.3 times higher than those in ice phase. On the other hand, HPI did not show an obvious distribution trend between liquid and ice phases. At the sampling point 4, the DOC value of HPI in ice phase was higher than that in liquid phase, while at the sampling points 1, 2, and 6, it was just the opposite. As shown in Fig. 3(a), the two hydrophobic fractions, i.e., HPO-A and HPO-N, alone constituted as much as 49.5%~69.5% of the total DOC (the sum of DOC for the five fractions) in liquid phase, indicating that the DOM in river waters was dominated by hydrophobic compounds. Among the five fractions in liquid phase, the DOC value of HPO-A was the highest with the range of 1.9~4.8 mg/L, comprising 29.0%~43.0% of the total DOC. On the contrary, the DOC value of HPI was the lowest, accounting for 1.2%~3.8%. The DOM-fraction distribution in ice phase was consistent with that in liquid phase (Fig. 3). Although HPO-A also ranked first in ice phase, its proportion decreased to 12.2%~37.0%. The contribution of HPI to the total DOC was still the lowest in ice phase. However, it increased to 2.5%~11.2%. The results indicated that DOM fractions differed in the partitioning behavior in liquid and ice phases during freezing processes of water, which was mainly attributed to their different physical/chemical properties, e.g., polarity, and molecular weight, etc. The five DOM fractions in this study were fractionated based on adsorption affinity for XAD-8 and XAD-4 resins, and the polarity of DOM fractions can be ranked as follows: hydrophobic fractions > transphilic fractions > HPI [23–25]. Polar molecules commonly have stronger affinity for water molecules thus making it more difficult to be rejected from the ice phase when the water freezes up, as compared with non-polar molecules [26]. According to Hua and Reckhow [25], HPO-A mainly consists of humic acid and fulvic acid generally with high molecular weight, whereas HPI is primarily comprised of carbohydrates, proteins, amino acids, and uronic acids, which are commonly characterized by low molecular weight. It is considered that the size of the impurities could affect their ability to integrate into the ice phase; the impurities with smaller size might be more easily incorporated into the ice structure in the freeze concentration than those with larger size [27–29]. Hence, the increased relative contents of HPI in DOM in ice phase relative to those in liquid phase might be attributed to its higher polarity and lower molecular weight in comparison with the other four fractions. On the other hand, the low polarity and high molecular weight of HPO-A might be responsible for its decreased relative contents in DOM in ice phase relative to those in liquid phase.

3.3 UV_{254} and SUVA of DOM fractions in liquid and ice phase

UV_{254} is absorbance of ultraviolet light at 254 nm, which was mainly caused by electron-rich sites, such as aromatic functional groups and double-bonded C groups, in the DOM molecule [30]. As shown in Fig. 4a, among five fractions, UV_{254} for HPO-A was the highest in liquid phase (3.9~11.0 m^{-1}), and TPI-A ranked second (0.6~5.4 m^{-1}). These two fractions alone constituted as much as 89.2%~97.0% of the total UV_{254} (the sum of UV_{254} for the five fractions). UV_{254} for neutral fractions (HPO-N and TPI-N) were relatively low, only accounting for 1.6%~5.0% of the total UV_{254}. HPO-A and TPI-A in ice phase also exhibited relatively high UV_{254} values, in the range of 0.6~9.7 m^{-1} and 0.5~7.3 m^{-1}, respectively (Fig. 4b). The sum of their contributions to the total UV_{254} in ice phase was 66.9%~95.2%, slightly lower than that in liquid phase. On the contrary, the contribution

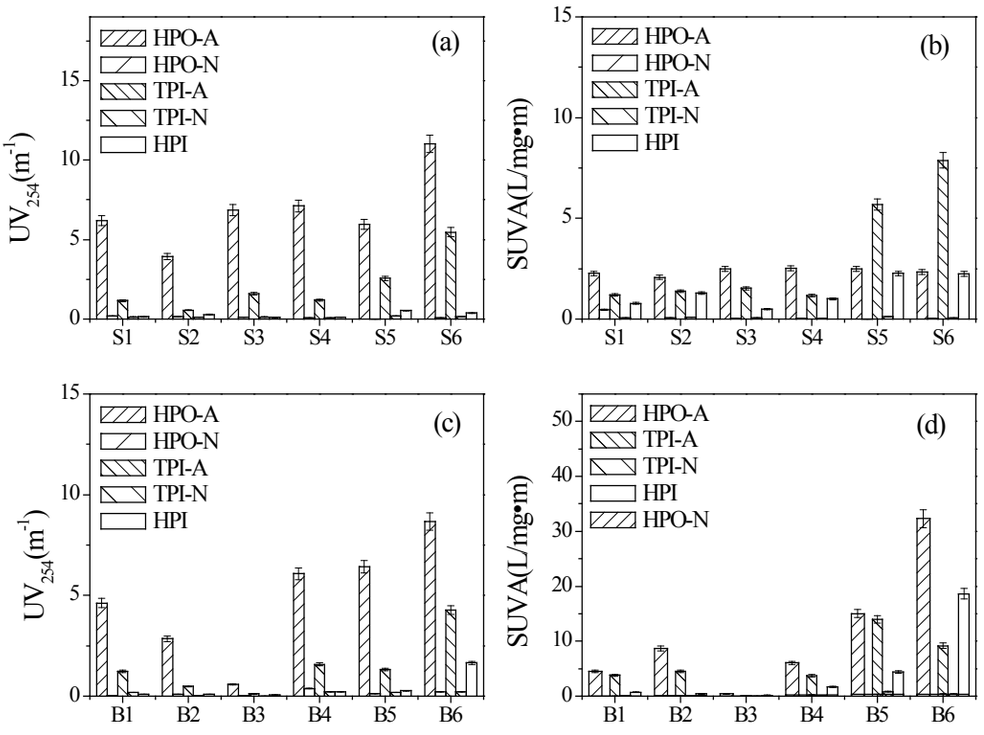

Fig. 4. UV_{254} (a) and SUVA (b) for DOM fractions in water samples, and UV_{254} (c) and SUVA (d) for DOM fractions in ice samples in the North Canal during icebound season.

of HPO-N, TPI-N and HPI to the total UV_{254} in ice phase was higher than that in liquid phase. It was also noticed that UV_{254} for HPO-A in liquid phase was about 1.1~11.7 times that in ice phase, suggesting that conjugated double bond and/or benzene ring structure in HPO-A was more easily to be concentrated in liquid phase, as compared with the bulk HPO-A. As shown in Table 2, the variation trend of UV_{254} along the direction of water was inconsistent with that of DOC in both liquid and ice phases. For example, in both liquid and ice phases, DOC significantly decreased whiles UV_{254} significantly increased, along the river reach from S4 to S5, which implied high relative contents of organics with conjugated double bond or benzene structures at the sampling point 5.

SUVA reflects the relative aromaticity of organics [3]. As shown in Fig. 4, except for S5 and S6 in which SUVA for TPI-A was the highest among the five fractions, SUVA for HPO-A was higher than that for other fractions in all samples, while SUVA for the two neutral fractions were the lowest in all samples. These results suggested that, among five fractions, HPO-A generally had relatively high content of organics containing conjugated double bond or benzene structures whereas neutral fractions exhibited low aromaticity. Except for the sample point 3, SUVA for acidic fractions, i.e., HPO-A and TPI-A, in ice phase was higher than that in liquid phase at each sampling point. The results suggested that those materials with high aromaticity in HPO-A and TPI-A were more likely to enter ice phase during the freezing processes of water.

3.4. Fluorescence spectra of DOM fractions in liquid and ice phase

EEM spectra for DOM fractions in liquid phase at all sampling points were shown in Fig. 5. In the fluorescence spectra of HPO-A and TPI-A at each sampling point, the aromatic protein-like peak II, as well as humic and fulvic acid-like peaks were observed. The fluorescence spectra of HPO-N and TPI-N in S1~S6 showed the aromatic protein-like fluorescence peak II. HPI at each sampling point exhibited the humic and fulvic acid-like fluorescence peaks.

EEM spectra for DOM fractions in ice phase at each sampling point were shown in Fig. 6. The fulvic and humic acid-like peaks were obviously found in the spectrum of HPO-A at each sampling point. The specra of HPO-N, TPI-N and HPI in B1~B6 had the aromatic protein-like fluorescence peak II. The aromatic protein-like fluorescence peak II, and fulvic and humic acid-like peaks, were observed in the spectra of TPI-A at all sampling points.

Since each sample was diluted to same DOC concentration when fluorescence spectra were obtained, all $\Phi_{i,n}$ and $\Phi_{T,n}$ values, shown in Figs. 7 and 8, were obtained by multiplying DOC by the fluorescence intensity calculated from FRI, representing the amount of fluorescent materials. This study plused $\Phi_{aromatic\ protein\text{-}like\ I}$ and $\Phi_{aromatic\ protein\text{-}like\ II}$ to represent the cumulative aromatic protein-like fluorescence, with $\Phi_{aromatic\ protein\text{-}like}$.

As shown in Fig. 7, $\Phi_{aromatic\ protein\text{-}like}$ made the greatest contribution to $\Phi_{T,n}$, accounting for about 79.5%~84.8%

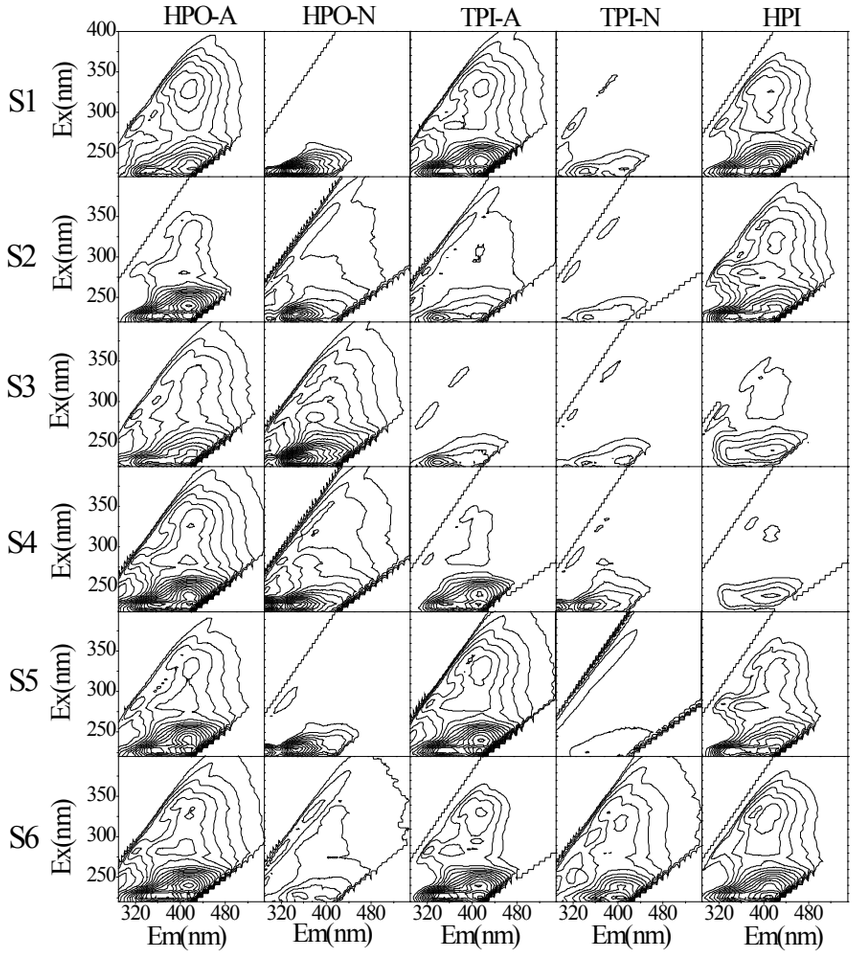

Fig. 5. EEM spectra for DOM fractions in water samples in the North Canal during icebound season.

of $\Phi_{T,n}$. Then $\Phi_{humic\ acid\text{-}like}$ ranked second, and $\Phi_{fulvic\ acid\text{-}like}$ and $\Phi_{SMP\text{-}like}$ made the lowest. It was reported that the excitation wavelength of protein-like fluorescent materials is in the ultraviolet range, with high photon yield. Thus, their fluorescence are easy to be detected, and the intensity is relatively high [31]. Baker and Inverarity [32] believed that protein-like fluorescent materials in the natural water were mainly originated from residues of microorganisms and phytoplankton as well as extracellular enzymes secreted by microorganisms. And the low temperature and DO in water during icebound season made the life activities of microorganisms and phytoplankton to be restrained, thus inhibiting the degradation of protein-like fluorescent materials. As a result, $\Phi_{aromatic\ protein\text{-}like}$ exhibited higher values than the other $\Phi_{i,n}$ values. It was also found that $\Phi_{SMP\text{-}like}$ and $\Phi_{humic\ acid\text{-}like}$ values of HPO-A and TPI-A were relatively high, while those of HPO-N and TPI-N were relatively low. Along the direction of water, for each fraction, the variation extent of $\Phi_{i,n}$ and $\Phi_{T,n}$ was not consistent with that of DOC in liquid phase. For example, from the sampling point 1 to 2, the DOC value of HPO-A in liquid phase decreased by 31.0%, while its $\Phi_{aromatic\ protein\text{-}like} > \Phi_{fulvic\ acid\text{-}like} > \Phi_{SMP\text{-}like} > \Phi_{humic\ acid\text{-}like}$ and $\Phi_{T,n}$ values only decreased by 10.0%, 10.9%, 9.1%, 8.0% and 10.1%, respectively. In addition, $\Phi_{i,n}$ of each fraction in liquid phase did not follow the same variation trend along the direction of water. These results implied that the degradation mechnisms for fluorescent materials might be different from those for non-fluorescent compounds, and the degradation mechnisms for different typies of fluorescent materials might be different from each other.

As shown in Fig. 8, the $\Phi_{i,n}$ values of DOM fractions in each ice sample could be ranked as follows: $\Phi_{aromatic\ protein\text{-}like} > \Phi_{SMP\text{-}like} > \Phi_{fulvic\ acid\text{-}like} > \Phi_{humic\ acid\text{-}like}$. Among $\Phi_{i,n}$, $\Phi_{aromatic\ protein\text{-}like}$ still made the greatest contribution to $\Phi_{T,n}$, accounting for about 79.9%~85.9% of $\Phi_{T,n}$. The variation trend of $\Phi_{i,n}$ of DOM fractions in ice phase along the direction of water was similar to that in liquid phase. However, it was inconsistent with that of DOC. For example, $\Phi_{aromatic\ protein\text{-}like}$ of HPO-A in B1 was 1.2 times that in S1, while DOC of HPO-A in B1 was 0.4 times that in S1. This might be attributed the differences between water/ice partitioning properties of fluorescent materials and non-fluorescent compounds.

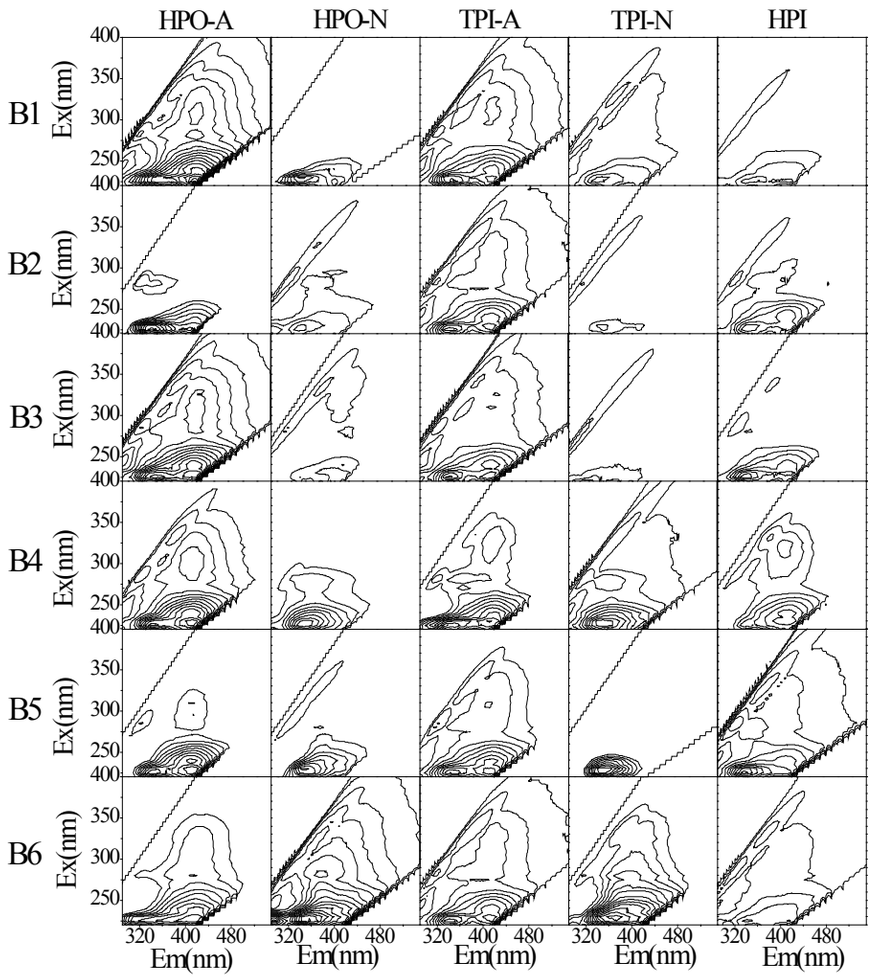

Fig. 6. EEM spectra for DOM fractions in ice samples in the North Canal during icebound season.

3.5. THMFP of DOM fractions in liquid and ice phase

THMFP is often the term employed to indicate the amount of THMs that could be produced during the chlorination process, and could indirectly represent the amount of THM precursors in water samples. Because THMFP is dependent upon DOC concentration, the reactivity of DOC is also reported in terms of specific THMFP (STHMFP), that is, micrograms of THMFP formed per milligram of DOC precursor material in the water [33].

As shown in Fig. 9, HPO-A, HPO-N and TPI-N showed relatively high THMFP values in liquid phase, and they collectively accounted for 79.5%~93.4% of the total THMFP (the sum of THMFP for five fractions). On the other hand, HPI had the lowest THMFP values in liquid phase, only accounting for 0.5%~3.1% of the total THMFP. These results suggested that HPO-A, HPO-N and TPI-N were the main of THM precursors. The contributions of HPO-A, HPO-N and TPI-N to THMFP in ice phase were still high, but the sum of their contributions decreased to 67.1%~90.8%. THMFP of HPI was still relatively low in ice phase, but its contribution to the total THMFP increased to 4.6%~23.0%. As shown in Fig. 9 (d), STHMFP of HPI in ice phase was higher than that of the other four fractions, which suggested that HPI had higher chlorine reactivity to produce THMs. However, DOC of HPI in ice phase was quite low. As a result, its THMFP was lower than that of the other fractions. THMFP of HPO-A, TPI-A, HPO-N and TPI-N in liquid phase was 2.5~11.5 times, 1.1~4.5 times, 1.1 ~7.5 times and 1.7~5.1 times that in ice phase, respectively. On the contrary, THMFP of HPI in liquid phase was lower than that in ice phase.

It was reported that SUVA could reflect the halogenated activity of organic matter [3]. However, SUVA was found not to be a good surrogate parameter for monitoring THMFP in this study. For example, HPI exhibited the highest STHMFP value in ice phase, while its SUVA value was generally lower than that of HPO-A and TPI-A. In addition, no linear relationship was found between THMFP of DOM fractions and their $\Phi_{i,n}/\Phi_{T,n}$ values in both liquid and ice phases (R^2 = 0~0.57, $p < 0.01$).

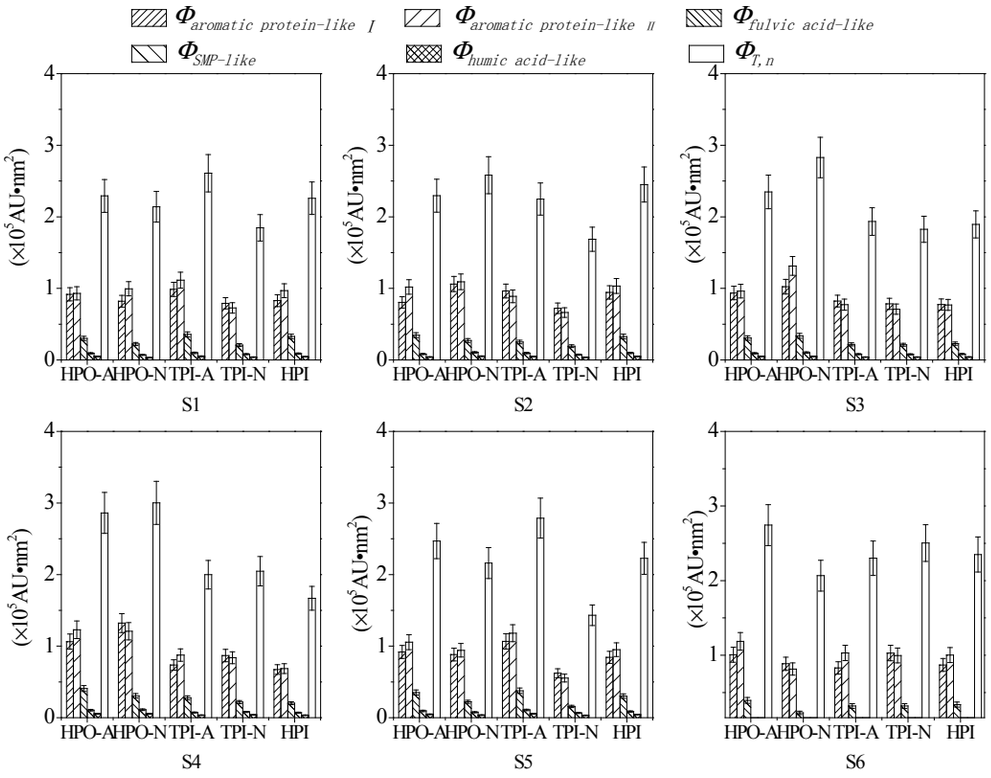

Fig. 7. $\Phi_{i',n}$ and $\Phi_{T,n}$ for DOM fractions in water samples in the North Canal during icebound season.

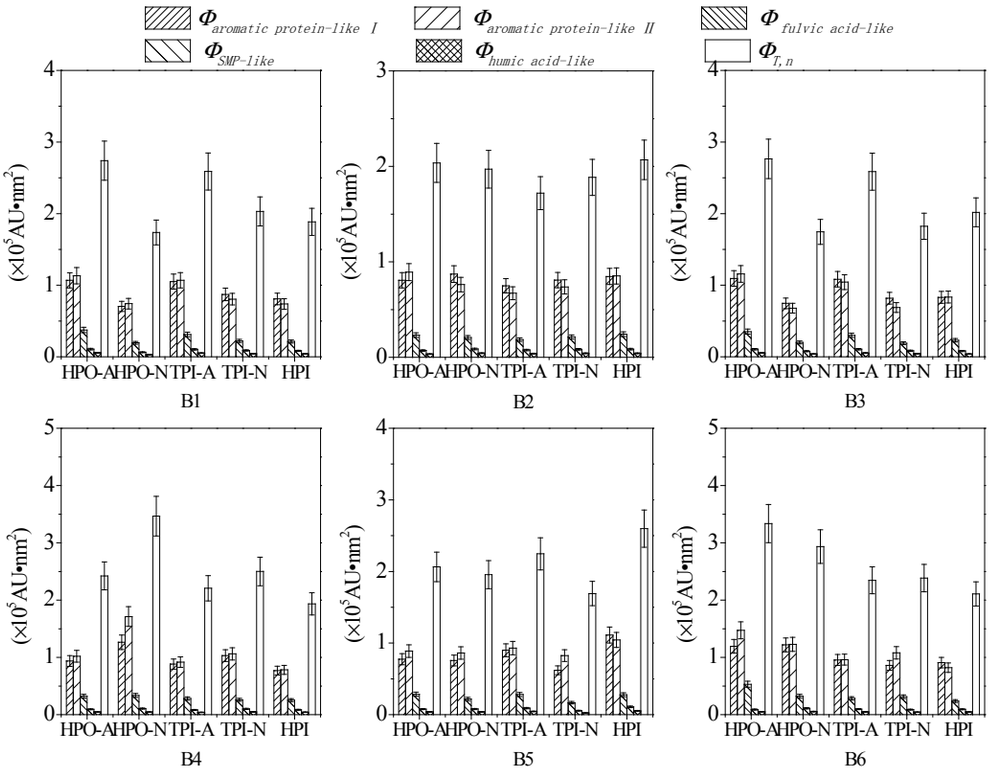

Fig. 8. $\Phi_{i',n}$ and $\Phi_{T,n}$ for DOM fractions in ice samples in the North Canal during icebound season.

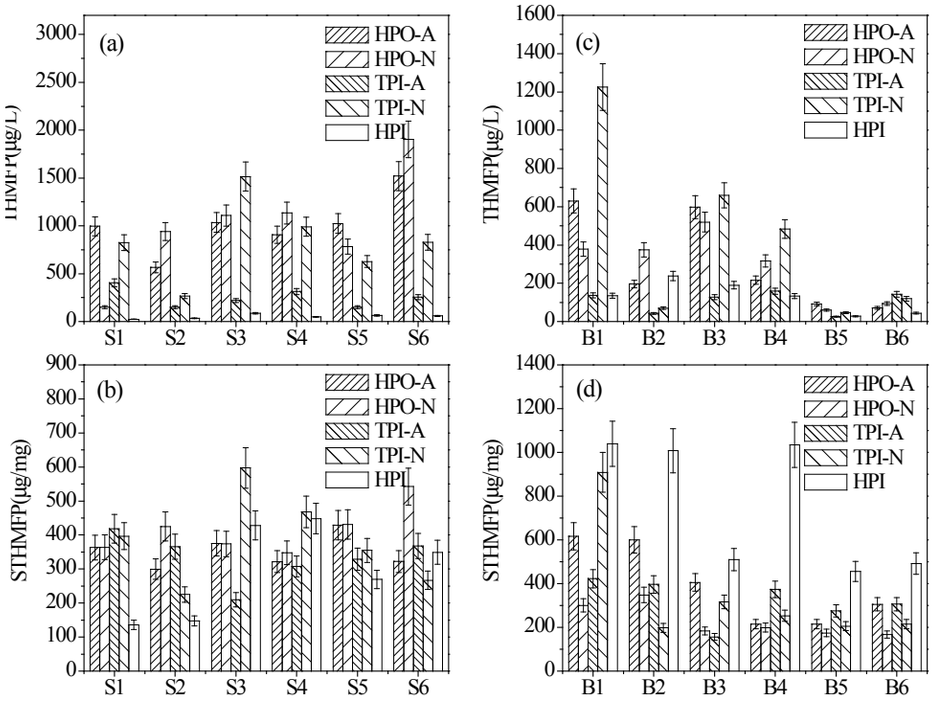

Fig. 9. THMFP (a) and STHMFP (b) for DOM fractions in water samples, and THMFP (c) and STHMFP (d) for DOM fractions in ice samples in the North Canal during icebound season.

4. Conclusions

1. The concentration of DOM in ice phase was 0.2~0.8 times that in liquid phase. In each sampling point, DOC values of HPO-A, TPI-A and TPI-N in liquid phase were higher than those in ice phase.
2. The sum of UV_{254} of HPO-A and TPI-A accounted for 89.2%~97.0% and 66.9%~95.2% of the total UV_{254} in liquid and ice phase, respectively.
3. The variation trend of $\Phi_{i,n}$ of DOM fractions in ice phase along the direction of water was similar to that in liquid phase. However, it was inconsistent with that of DOC.
4. THMFP of HPO-A, HPO-N and TPI-N in both liquid and ice phases was relatively higher while that of TPI-A and HPI was relatively lower. THMFP of HPO-A, TPI-A, HPO-N and TPI-N in liquid phase was 2.5~11.5 times, 1.1~4.5 times, 1.1 ~7.5 times and 1.7~5.1 times that in ice phase, respectively. On the contrary, THMFP of HPI in liquid phase was lower than that in ice phase.

Acknowledgements

The work was supported by the National Natural Science Foundation of China (No. 21107039), the Science and Technology Research Project of Liaoning Provincial Education Department (No. L2011002), the Science and Technology Plan Project of Liaoning Province (No. 2011230009), and the Major Science and Technology Program for Water Pollution Control and Treatment (No. 2012ZX07505-001-01).

References

[1] C.T. Chlou, R.L. Malcolm, T.I. Brlnton, D.E. Klle, Water solubility enhancement of some organic pollutants and pesticides by dissolved humic and fulvic acids, Environ. Sci. Technol., 20 (1986) 502–508.
[2] P.Q. Fu, F.C. Wu, C.Q. Liu, F.Y. Wang, W. Li, L.X. Yue, Q.J. Guo, Fluorescence characterization of dissolved organic matter in an urban river and its complexation with Hg (II), Appl. Geochem., 22 (2007) 1668–1679.
[3] J.A. Leenheer, J.P. Croué, Characterizing dissolved aquatic organic matter, Environ. Sci. Technol., 37 (2003) 18A–26A.
[4] B. Panyapinyopol, T.F. Marhaba, V. Kanokkantapong, P. Pavasant, Characterization of precursors to trihalomethanes formation in Bangkok source water. J. Hazard. Mater., 120 (2005) 229–236.
[5] L.B. Barber, J.A. Leenheer, T.I. Noyes, E.A. Stiles, Nature and transformation of dissolved organic matter in treatment wetlands. Environ. Sci. Technol., 35 (2001) 4805–4816.
[6] Y. Yamashita, E. Tanoue, Chemical characterization of protein-like fluorophores in DOM in relation to aromatic amino acids. Mar. Chem., 82 (2003) 255–271.
[7] W. Chen, P. Westerhoff, J.A. Leenheer, K. Booksh, Fluorescence excitation–emission matrix regional integration to quantify spectra for dissolved organic matter, Environ. Sci. Technol., 37 (2003) 5701–5710.
[8] F.C. Marhuenda-Egea, E. Martínez-Sabater, J. Jordá, R. Moral, M.A. Bustamante, C. Paredes, M.D. Pérez-Murcia, Dissolved organic matter fractions formed during composting of winery and distillery residues: evaluation of the process by fluorescence excitation–emission matrix. Chemosphere, 68 (2007) 301–309.
[9] C. Neal, H.P. Jarvie, P.J.A. Withers, B.A. Whitton, M. Neal, The strategic significance of wastewater sources to pollutant phosphorus levels in English rivers and to environmental management for rural, agricultural and urban catchments, Sci. Total Environ., 408 (2010) 1485–1500.

[10] P. Weyrauch, A. Matzinger, E. Pawlowsky-Reusing, S. Plume, D.v. Seggern, B. Heinzmann, K. Schroeder, P. Rouault, Contribution of combined sewer overflows to trace contaminant loads in urban streams, Water Res., 44 (2010) 4451–4462.
[11] J.M. Evans, S.D. Schiller, Application of microclimate studies in town planning: A new capital city, an existing urban district and urban river front development, Atmos. Environ., 30 (1996) 361–364.
[12] R.J. Hou, H.M. Li, Mathematical model describing BOD-DO dynamics for rivers in northern China during freezing season, Acta. Sci. Circumstantiae., 2 (1982) 113–116.
[13] B. Garban, D. Ollivon, A. Jaïry, A.M. Carru, A. Chesterikoff, The role of phytoplankton in pollutant transfer processes in rivers. Example of River Marne (France), Biogeochem., 44 (1999) 1–27.
[14] G.R. Aiken, D.M. Mcknight, K.A. Thorn, E.M. Thurman, Isolation of hydrophilic organic acids from water using nonionic macroporous resins, Org. Geochem., 18 (1992) 567–573.
[15] J. Chen, S. Xue, Y.Z. Lin, C. Wang, Q. Wang, Q. Han, Effect of freezing–thawing on dissolved organic matter in water, Desal. Water Treat., 57 (2016) 17230–17240.
[16] P.D. Wentzell, S.S. Nair, R.D. Guy, Three-way analysis of fluorescence spectra of polycyclic aromatic hydrocarbons with quenching by nitromethane, Anal. Chem., 73 (2001)1408–1415.
[17] S. Xue, Q.L. Zhao, L.L. Wei, Y.T. Song, M. Tie, Fluorescence spectroscopic characterization of dissolved organic matter fractions in soils in soil aquifer treatment, Environ. Monit. Assess., 185 (2013) 4591–4603.
[18] Y.P. Liu, D.H. Wang, Strengthened the pollution treatment in the period of ice sealed is the key of the Songhua River s traditional, Environ. Sci. Manage., 31 (2006) 37–38.
[19] X.E. Wang, D.M. Dong, W.J. Zhao, J. Li, H.L. Zhang, Y.G. Du, Reduction mode of organic pollutants in rivers during the ice-bound season, J. Jilin Univ. : Nat. Sci. Ed., 41 (2003) 392–395.
[20] Q.H. Zheng, Y.Q. Wu, Y.G. Zhang, Models for estimating pollutant reduction in rivers during freezing period, J. B. Normal Univ. : Nat. Sci. Ed., 42 (2006) 615–617.
[21] S. Xue, Y. Wen, X.J. Hui, L.N. Zhang, Z.H. Zhang, J. Wang, Y. Zhang, The migration and transformation of dissolved organic matter during the freezing processes of water, J. Environ. Sci., 27 (2015)168–178.
[22] O. Lorain, P. Thiebaud, E. Badorc, Y. Aurelle, Potential of freezing in wastewater treatment: soluble pollutant applications, Water Res., 35 (2001) 541–547.
[23] A.T. Chow, F. Guo, S. Gao, R. Breuer, Size and XAD fractionations of trihalomethane precursors from soils, Chemosphere, 62 (2006) 1636–1646.
[24] J. Chen, B. Gu, E.J. LeBoeuf, H. Pan, S. Dai, Spectroscopic characterization of the structural and functional properties of natural organic matter fractions, Chemosphere, 48 (2002) 59–68.
[25] G.H. Hua, D.A. Reckhow, Characterization of disinfection byproduct precursors based on hydrophobicity and molecular size, Environ. Sci. Technol., 41 (2007) 3309–3315.
[26] J.J. Chen, X.N. Fei, Y.G. Jiang, G.Y. Du, C. Jiang, A comparison study on the removal of the pollutants in wastewater treated by freezing separation, Environ. Sci. Manage., 35 (2010) 96–98.
[27] R. Halde, Concentration of impurities by progressive freezing, Water Res., 14 (1980) 575–580.
[28] W. Gao, Y. Shao, Freeze concentration for removal of pharmaceutically active compounds in water, Desalination, 249 (2009) 398–402.
[29] F. Belén, S. Benedetti, J. Sánchez, E. Hernández, J.M. Auleda, E.S. Prudêncio, J.C.C. Petrus, M. Raventós, Behavior of functional compounds during freeze concentration of tofu whey, J. Food Eng., 116 (2013) 681–688.
[30] D.M. Quanrud, J. Hafer, M.M. Karpiscak, H.M. Zhang, K.E. Lansey, R.G. Arnold, Fate of organics during soil-aquifer treatment: sustainability of removals in the field, Water Res., 37 (2003) 3401–3411.
[31] X.S. He, B.D. Xi, Z.M. Wei, Y.H. Jiang, Y. Yang, D. An, J.L. Cao, H.L. Liu, Fluorescence excitation–emission matrix spectroscopy with regional integration analysis for characterizing composition and transformation of dissolved organic matter in landfill leachates, J. Hazard. Master., 190 (2011) 293–299.
[32] D.A. Baker, R. Inverarity, Protein-like fluorescence intensity as a possible tool for determining river water, Hydrol. Pro., 18 (2004) 2927–2945.
[33] R.P. Galapate, A.U. Baes, M. Okada, Transformation of dissolved organic matter during ozonation effects on trihalomethane for mation potential, Water Res., 35 (2001) 2201–2206.